first order one may approximate the valence-band electron density of states of amorphous GeTe as a sum of those of amorphous Ge and of amorphous Te.[13] Such a model is based on the structural similarity to amorphous GeTe containing amorphous Ge-like and amorphous Te-like bonds. It is found that the *s* levels of this model are broader than those observed.[13] This can be explained by the presence of Ge-Te bonds in amorphous GeTe. Any tendencies to bring *s* orbitals lying at different energies together tends to weaken the resonant bonding, thereby making the levels sharper.

However, the similarities in the XPS of the amorphous and crystalline forms suggests that also the density of states of the crystalline form can serve as an adequate first approximation for the density of states of the amorphous form. The crystalline form is structurally unlike the amorphous form and application of such a model is not by any means *a priori* obvious. Nevertheless, we can explain the broadening of the *s* levels in the amorphous form by tendencies of like atoms to be nearest neighbors.

We conclude that valence bands of amorphous and crystalline GeTe are similar even though their structures are significantly different. This suggests that within the resolution of nonmonochromatized electron spectroscopy for chemical analysis (~ 1.5 eV), the density of valence states of a given compound is essentially unaffected by changes in the long- and short-range order.

Useful discussions with H. von Heyszenau and M. Thorpe are gratefully acknowledged. We also thank Dr. E. Schönherr for preparing the GeTe sputtering target, and Mr. G. Krutina for assistance in making the measurements.

*On leave from Aerospace Research Laboratories, Wright-Patterson Air Force Base, Dayton, Ohio 45433.

[1]A. Bienenstock, F. Betts, and S. R. Ovshinsky, J. Non-Cryst. Solids 2, 347 (1970).

[2]F. Betts, A. Bienenstock, and S. R. Ovshinsky, J. Non-Cryst. Solids 4, 554 (1970).

[3]D. B. Dove, M. B. Heritage, K. L. Chopra, and S. K. Bahl, Appl. Phys. Lett. 16, 138 (1970).

[4]D. B. Dove, T. Chang, and B. Molnar, J. Non-Cryst. Solids 8-10, 376 (1972).

[5]N. J. Shevchik, to be published.

[6]K. L. Chopra and S. K. Bahl, J. Appl. Phys. 40, 4171 (1969).

[7]S. K. Bahl and K. L. Chopra, J. Appl. Phys. 41, 2196 (1970).

[8]M. H. Brodsky and P. Stiles, Phys. Rev. Lett. 25, 798 (1970).

[9]C. J. Vesely and D. W. Langer, Phys. Rev. B 4, 451 (1971).

[10]M. Cardona, C. M. Penchina, E. E. Koch, and P. Y. Yu, Phys. Status Solidi (b) 53, 327 (1972).

[11]F. Betts, A. Bienenstock, and C. W. Bates, J. Non-Cryst. Solids 8-10, 364 (1972).

[12]G. B. Fisher and W. E. Spicer, J. Non-Cryst. Solids 8-10, 978 (1972).

[13]N. J. Shevchik, J. Tejeda, D. W. Langer, and M. Cardona, to be published.

[14]G. B. Fischer and W. E. Spicer, private communication.

[15]Y. W. Tung and M. L. Cohen, Phys. Rev. 180, 823 (1969); M. Cohen, Y. W. Tung, and P. B. Allen, J. Phys. (Paris), Colloq. 29, C4-62 (1968).

[16]F. Herman, R. L. Kortum, J. B. Ortenburger, and P. Van Dyke, J. Phys. (Paris), Colloq. 29, C4-62 (1968).

[17]L. Pauling, *Nature of the Chemical Bond* (Cornell Univ. Press, Ithaca, New York, 1960), 3rd ed.

Spin-Flop Domains in MnF_2 †

A. R. King and D. Paquette
Department of Physics, University of California, Santa Barbara, California 93106
(Received 27 November 1972)

An intermediate state is shown to exist between the antiferromagnetic and spin-flop states of antiferromagnetic MnF_2. This state consists of alternate thin-slab domains of antiferromagnetic and spin-flop material. Experimental evidence includes NMR, Faraday rotation, optical-absorption spectroscopy, and photographs of the domain structure. A molecular field model is used to calculate the field width of the domain region and the physical width of the domains. Reasonable numerical agreement is found.

In studying the F^{19} NMR near the spin-flop (SF) transition in antiferromagnetic MnF_2, evidence was found for a new type of intermediate state between the antiferromagnetic (AF) and SF states. In a narrow region of magnetic field (≈ 1 kG) near SF, the NMR frequency is completely indepen-

dent of applied field. Since similar screening is observed in the NMR in ferromagnets exhibiting a domain structure, we postulate a new type of domain structure, in which alternate thin slablike domains are either AF or SR. The SF transition, which would otherwise be first order, proceeds gradually, with the width of the SF domains growing at the expense of the AF as the field is increased.

For further confirmation of the existence of these domains, we have studied the optical spectroscopy of MnF_2 in the region near SF. A particular sharp absorption line[1] is found to split in the region of interest, indicating that AF and SF states exist simultaneously. The Faraday rotation (FR)[2] in MnF_2, rather than abruptly changing at SF, changes gradually in the domain region.

As the most convincing proof of the existence of these domains, we have taken photographs which clearly show the appearance of slablike domains at a particular field. In the course of this work we have learned of several papers on this subject[3] in which it was shown that magnetization changes as a function of field near SF are consistent with a domain model. Their observed "jumps" of the magnetization were interpreted as creation or annihilation of domain walls.

We have made a molecular-field–model calculation which describes the extent of the domain region, the screening of the local fields, the fraction of SF and AF material, and also the domain width, all in satisfactory agreement with the data.

The experiments were done in a superconducting solenoid at $T = 4.2$°K. Field measurements were made with magnetoresistance and NMR magnetometers. Since SF is extremely sensitive to sample orientation,[4] all sample holders had tilting platforms on which samples were mounted and could be aligned, *in situ*, to better than $\frac{1}{6}$ deg.

(A) For the NMR experiments a roughly ellipsoidal sample ($3.2\times 7.9\times 3.2$ mm^3) was mounted in a broad-band, untuned slow-wave structure used with a broad-band NMR detector, which allowed continuous monitoring of the NMR while scanning the field. Figure 1 shows data on the lower branch of the F^{19} NMR in the region near SF. Below a critical value of the field, $H_c = 92.4$ kG, the NMR frequency has the usual slope $\gamma = 4.005$ kHz/Oe for F^{19}. However, as the field is increased above H_c, the frequency abruptly becomes field independent, while the NMR intensity decreases monotonically to zero over an interval

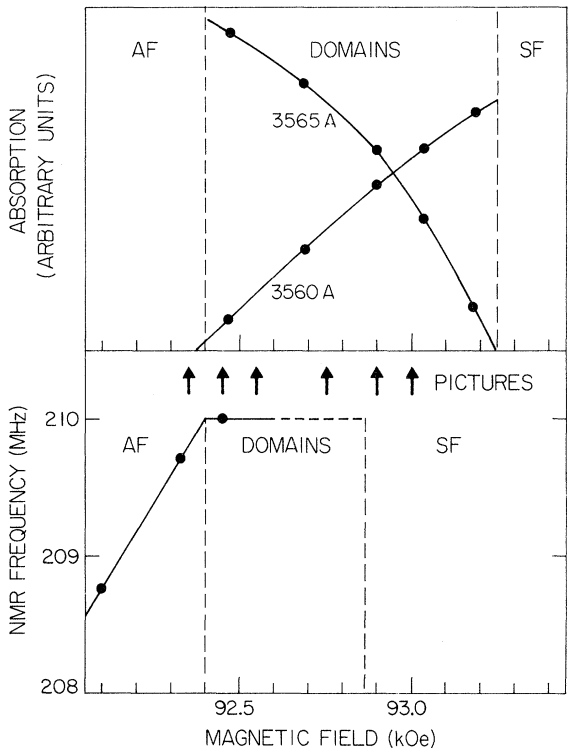

FIG. 1. Optical-absorption intensity of $\lambda = 3560$-Å (SF), 3565-Å (AF) transitions, location of photographs, and F^{19} NMR frequency as a function of applied magnetic field in the domain region.

of several hundred gauss.

(B) The optical system uses a Xe lamp and a monochromator where the output beam is focused through a Dewar window onto the sample. A sample-holder–mounted lens collects transmitted light and focuses an image of the sample on either a photomultiplier or photographic film for spectroscopy or photography. For the optical experiments this sample was a flat disk, 0.200 in. deep $\times 0.050$ in. thick, with the c axis perpendicular to the flat faces.

(C) With the sample inserted between polarizing filters with a relative angle of 45°, we can detect variation in the FR through intensity changes. With well-aligned samples, a field scan in the vicinity of H_c shows three distinct FR regions. In the AF and SF regions the FR has nearly the same linear field dependence, while in the domain region it has opposite slope, with sharp breaks in slope at the end points of the regions. With samples less well aligned, the intermediate region widens, the sharp breaks at the end points become rounded, and the slope decreases.

This latter fact is used to advantage to align

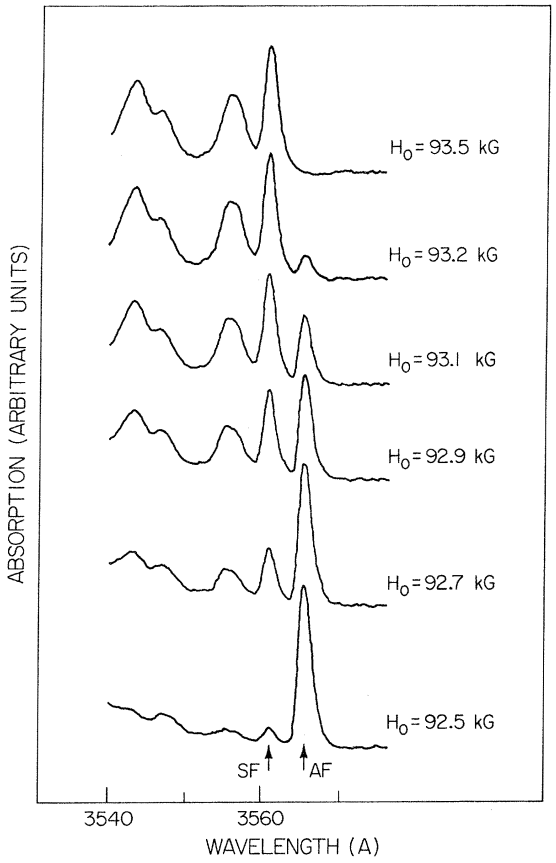

FIG. 2. Optical absorption in the region around 3560 Å as a function of field in the domain region. The 3565-Å line corresponds to AF domains, the 3560-Å line and other structure to SF.

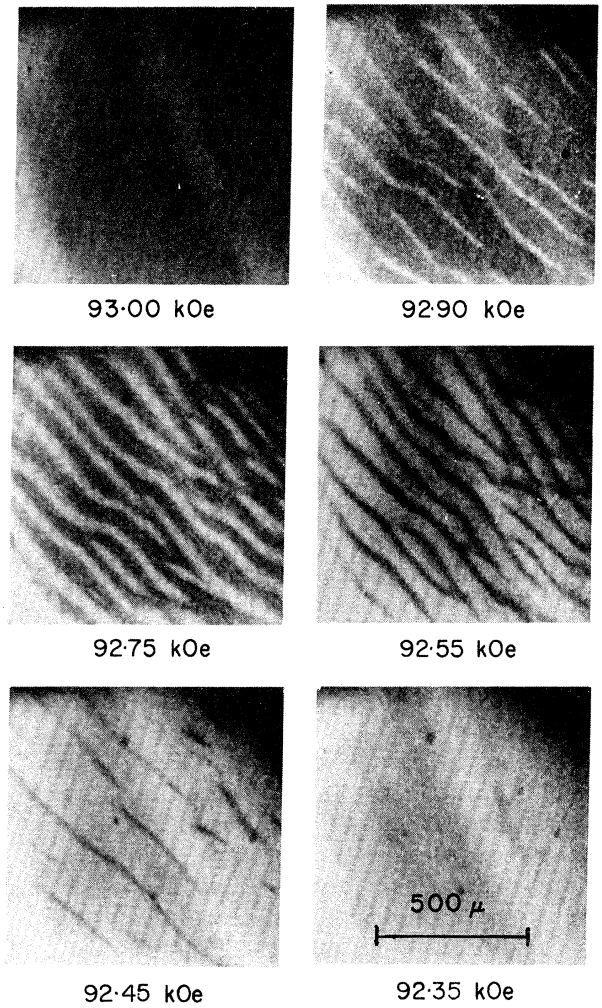

FIG. 3. Photographs of domain structure. The sample was illuminated with light of $\lambda = 3560$ Å, corresponding to the SF transition. SF regions appear dark; AF regions, light. Slab orientation is not along any major crystalline axis.

our samples, *in situ*. A modulation field is applied, the sample orientation is adjusted for maximum ac photomultiplier output, which corresponds to optimum alignment. This technique consistently yields alignment to better than $\frac{1}{6}$ deg.

(D) The largest changes in the optical-absorption spectrum near SF are shown by a group of narrow lines around 3560 Å,[1] which shift by about 5 Å. We have studied these transitions as a function of field around SF. Figure 2 shows some of our results. The line at 3565 Å (AF) decreases in intensity, while the line at 3560 Å (SF) increases in intensity as the field is increased through the domain region. The simultaneous presence of both AF and SF absorption lines clearly suggests the existence of domains. As shown in Fig. 1, the proportion of AF $(1-f)$ and SF material (f) can be determined by the relative intensities.

(E) The change in optical absorption at SF has made it possible to photograph the domain structure directly. Using 3560-Å light (SF absorption line) the SF regions absorb considerably more light than the AF ones. Consequently, the photographs in Fig. 3 show the SF domains darker than the AF. As the field is increased through the SF region, a few thin SF domains appear in the previously AF sample, then grow in width at the expense of the AF ones. Finally the AF domains become very thin and begin to disappear, leaving the sample completely SF.

The field locations of the photographs are indicated in Fig. 1. The low-field end of the domain region agrees well with the spectroscopy data, although the high-field photograph clearly

shows no domains at a field only 630 G higher, well within the domain region shown in the spectroscopy data. Possible reasons for this apparent discrepancy will be discussed later.

The general appearance of the domain structure is of parallel slablike domains although the waviness, branching, and free ends are not described by our simple model. Domain walls appear to be pinned, probably because of sample imperfections, since many walls remain in the same position through most of the field range. The observed average width of a domain, in the center of the domain region, is $d = 42$ μm.

We have used a molecular field model characterized by exchange and anisotropy fields H_e and H_a and *demagnetizing fields* to calculate the free energy of the AF, SF, and a domain state consisting of slabs. This domain state is found to be the lowest of these three in energy in a small region around the usual SF field.

We write the magnetic energy of a single, slab SF domain [N_z(slab) = 0, where N_z is the overall sample demagnetizing factor] aligned parallel to the macroscopic internal field $\vec{H}_m$,

$$E_{SF} = -H_m\chi_m + E_a.$$

χ_m is the macroscopic susceptibility [$\chi_m \cong \chi_\perp(\theta = \pi/2)$, defined below]; $E_a = ng\mu_B SH_a$, the anisotropy energy, $2n$ being the number of spins per unit volume. A fraction f of the sample is presumed to consist of narrow SF domains, uniformly distributed, so that H_m is uniform throughout the ellipsoidal sample. H_m is given by $H_m = H_0/(1 + fN_z\chi_m)$, yielding the energy of the domain state,

$$E_D = -H_0^2\chi_m f/2(1 + fN_z\chi_m) + fE_a.$$

H_0 is the applied field. Minimizing $E_D(f)$ gives $fN_z\chi_m H_{SF} = H_0 - H_{SF}$, where we have ignored demagnetizing corrections to the SF field and used $H_{SF} = (2H_eH_a - H_a^2)^{1/2}$. When $f = 0$, the first SF domain appears at $H_0 = H_{SF}$, independent of N_z. When $f = 1$, the last AF domain disappears at $H_0 = H_{SF}(1 + N_z\chi_m)$, giving the extent of the domain region as $\Delta H_D = H_{SF}N_z\chi_m$. In very thin samples ($N = 4\pi$), $\Delta H_D = 1200$ Oe. H_m is exactly screened over the domain region to the value $H_m = H_{SF}$.

Within a domain wall, the vector $\vec{L} = \vec{M}_+ - \vec{M}_-$ rotates through an angle θ ($0 < \theta \leq \pi/2$) from the c axis. Using the susceptibility[5]

$$\chi_\perp = 2g\mu_B S\sin\theta/(2H_e + H_a\cos 2\theta)$$

and the anisotropy energy

$$E_a = \tfrac{1}{2}ng\mu_B SH_a\sin^2\theta,$$

we calculate the energy of a thin slab with $\vec{L}$ rotated uniformly through the angle θ. We find, when $H_m = H_{SF}$ (anywhere in the domain region), that the values $\theta = 0$ (AF) and $\theta = \pi/2$ (SF) yield equal values of the energy. For intermediate values of θ, we find exact cancelation of the $\sin^2\theta$ terms, leaving only the much smaller term

$$E_a' = \tfrac{1}{4}ng\mu_B S(H_a^2/H_e)\sin^2 2\theta.$$

It is this anisotropy energy which stabilizes the 90° wall. It follows directly from the $\cos 2\theta$ term in $\chi_\perp$.

Using E_a', we follow standard calculations[6] for a ferromagnetic domain structure, with apt changes for SF domains. The specific wall energy ζ depends on the balance of exchange energy and E_a' in the wall. In a sample of thickness l, when AF and SF domains have equal width d ($f = \frac{1}{2}$), we find the magnetostatic energy $E_m = 0.43 \times \chi_m^2 H_{SF}^2 d$ obtained from the formation of domains to be $\frac{1}{4}$ that of the ferromagnetic case of thin planar, 180° domains. Minimizing the sum of E_m and the wall energy $\zeta l/d$ with respect to d yields $d = (\zeta l/0.43\chi_m^2 H_{SF}^2)^{1/2}$.

Each prediction of the theory can be compared with experimental results from one or more measurements. The exact screening of H_m is well verified by the NMR data of Fig. 1, within an experimental error of ± 2 G.

The predicted linear dependence of f on H can be compared with the spectroscopy data of Fig. 1. The curvature of the 3565-Å data and the different shapes of the two curves are not understood.

In the optical sample the field interval $\Delta H_D(N_z = 2.8\pi) = 830$ G, in excellent agreement with 850 G from the spectroscopy (Fig. 1). The discrepancy in the photography data (630 G) may be due to hysteresis effects, not yet studied, but indicated to some degree by the pinning of the domain walls. However, the good agreement of H_{SF} from all three measurements (Fig. 1) indicates too small an effect. Another possibility is the formation of bubble domains too small to be resolved in the photography, but seen in the spectroscopy.

Finally, we find adequate agreement between our calculated domain width of 13 μm and experimental result of 42 μm.

Further work is in progress on this and other samples to investigate hysteresis effects, sample misalignment effects, possible bubble domains, and the effect of sample thickness on do-

main width.

We wish to thank Professor V. Jaccarino for many helpful discussions and suggestions.

†Work supported in part by the National Science Foundation.

[1]D. S. McClure, in *Optical Properties of Ions in Crystals*, edited by H. M. Crosswhite and H. W. Moos (Interscience, New York, 1967), p. 257.

[2]M. F. Kharchenko and V. V. Eremenko, Fiz. Tverd. Tela 9, 1655 (1967), and 10, 1402 (1968) [Sov. Phys. Solid State 9, 1302 (1967), and 10, 1112 (1968)].

[3]K. L. Dudko, V. V. Eremenko, and V. M. Fridman, Zh. Eksp. Teor. Fiz. 61, 678, 1553 (1971) [Sov. Phys. JETP 34, 362, 828 (1972)].

[4]S. Foner, in *Magnetism*, edited by G. T. Rado and H. Suhl (Academic, New York, 1963), Vol. 1, Chap. 9.

[5]T. Nagamiya, K. Yosida, and R. Kubo, Advan. Phys. 4, 1 (1955) (or p. 38 for formula).

[6]S. Chikazumi, *Physics of Magnetism* (Wiley, New York, 1964), Chaps. 9–11.

(^{16}O, ^{12}C) and (^{6}Li, d) as α-Transfer Reactions

R. M. DeVries*

Département de Physique Nucléaire, Centre d'Etudes Nucleaires de Saclay, 91190–Gif sur Yvette, France

(Received 6 December 1972)

By means of a finite-range distorted-wave Born-approximation program which exactly includes recoil, α spectroscopic factors are extracted from the (^{6}Li, d) and (^{16}O, ^{12}C) reactions on ^{40}Ca. The production of ^{12}C*(2^{+}) is correctly predicted to be suppressed. The results are consistent with the assumption of an α-particle transfer as dominant in the two reactions.

The nature of the (^{16}O, ^{12}C) reaction is not well understood[1]; in particular, the internal state of the transferred four nucleons is not known although the reaction is usually referred to as an "α"-transfer reaction. In this paper the (^{16}O, ^{12}C) and the direct component of the (^{6}Li, d) reactions are assumed to proceed via the one-step transfer of an α particle, an assumption which seems fairly well established for the Li-induced reactions.[2] Two questions are answered: (a) Is the (^{16}O, ^{12}C) reaction quantitatively consistent with the (^{6}Li, d) reaction? (b) Why is the (^{16}O, ^{12}C*) reaction not observed on medium-mass targets?

Recent measurements of the (^{6}Li, d) reaction on ^{40}Ca[3] and ^{58}Ni[4] allow comparison with the spectra seen in the (^{16}O, ^{12}C)[5,6] reaction on the same targets. There appears to be an overall correlation between the strong levels produced in the two reactions. In this paper, finite-range distorted-wave Born-approximation (DWBA) calculations for the (^{6}Li, d) and (^{16}O, ^{12}C) reactions on ^{40}Ca are compared, this target being chosen because angular distributions exist for both reactions. It should be noted that zero-range DWBA calculations were made for the (^{6}Li, d) reactions, which reproduced the shapes of the angular distributions, but no absolute spectroscopic factors could be obtained. The (^{16}O, ^{12}C) reaction is not expected to be meaningfully treated with the zero-range or more sophisticated approximations unless they include recoil effects.[7] In this paper a DWBA formalism[8] is used which exactly includes recoil effects.

For a stripping reaction $A(a,b)B$, where $a=b+x$ and $B=A+x$, a transition amplitude may be written[8]

$$T \propto S_a^{1/2} S_B^{1/2} \int d^3r_a\, d^3r_b\, \chi_{aA}^{(+)}(\vec{r}_a) \langle \Psi_B(\vec{r}_{xA}) | V_{xb}(\vec{r}_{xb}) | \Psi_a(\vec{r}_{xb}) \rangle \chi_{bB}^{(-)}(\vec{r}_b). \quad (1)$$

In this expression χ is a distorted wave and the bracketed term is a form factor containing a final bound state Ψ_B and the potential V_{bx} used to generate the bound state Ψ_b.

The equation[9]

$$2N + L = \sum_{i=1}^{4} (2n_i + l_i) \quad (2)$$

determines the number of nodes N and the L value from the shell model n_i and l_i of each particle. The four nucleons are assumed to be in an internal 0s state with the known α binding energy. Table I lists the assumed shell-model configurations and resulting N and L values. Multi-particle-hole configurations in the ^{16}O(g.s.) are ignored, a procedure which is justified from analysis[12] of the reactions ^{12}C(^{6}Li, d)^{16}O and ^{16}O(d,

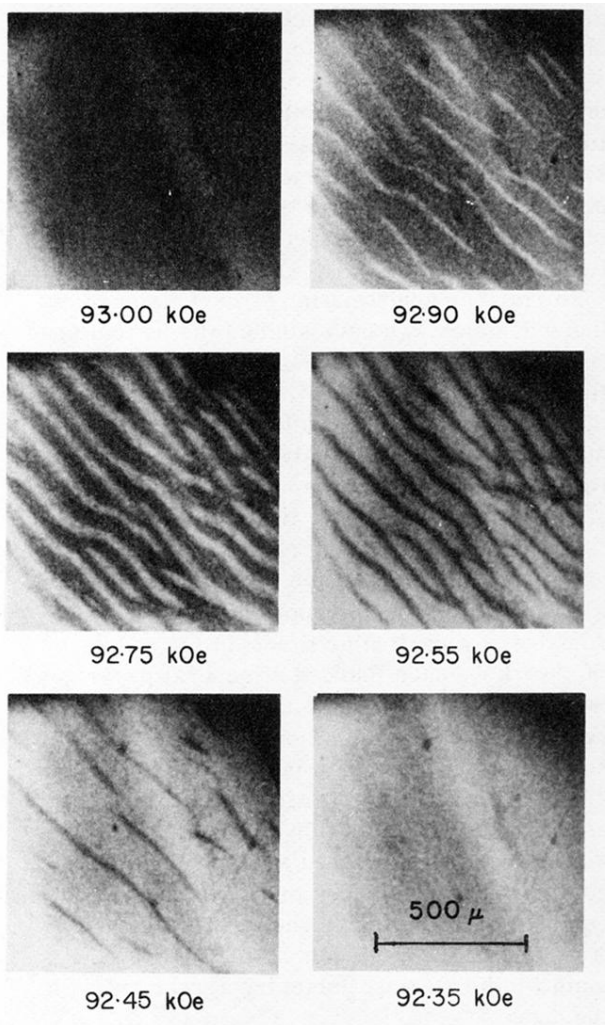

FIG. 3. Photographs of domain structure. The sample was illuminated with light of $\lambda = 3560$ Å, corresponding to the SF transition. SF regions appear dark; AF regions, light. Slab orientation is not along any major crystalline axis.